

## Article

# Affect of the Scattering Asymmetry by Structural Element of Thermal- or Environmental-Barrier Ceramics on Subsurface Radiant Overheating

Vladimir Merzlikin <sup>1,2,\*</sup> , Evgeny Safonov <sup>3</sup> , Andrey Kostyukov <sup>4</sup> , Svetlana Parshina <sup>2</sup>   
and Anna Dokukina <sup>1</sup> 

<sup>1</sup> Department of Economics of Industry, Plekhanov Russian University of Economics, Stremyanny, 36, 117997 Moscow, Russia

<sup>2</sup> Department of Technology and Equipment of Mechanical Engineering, Moscow Polytechnic University, Bolshaya Semenovskaya, 38, 111116 Moscow, Russia

<sup>3</sup> Faculty of Mechanical Engineering, Moscow Polytechnic University, Bolshaya Semenovskaya, 38, 111116 Moscow, Russia

<sup>4</sup> Department of Power Plants for Transport and Small-Scale Power Generation, Moscow Polytechnic University, Bolshaya Semenovskaya, 38, 111116 Moscow, Russia

\* Correspondence: merzlikinv@mail.ru

**Abstract:** The problem of the formation and estimation of a thermoradiant and temperature field in ceramics Thermal- Environmental-Barrier Coatings (TBC/EBC) has been considered with complex heat transfer but under the influence of the penetrating intense radiant component. The authors proposed to analyze not only TBC but also EBC from the point of view of the optics of semitransparent scattering and absorbing media in the range of  $\sim 0.4\text{--}4\ \mu\text{m}$  of external radiant action. This paradigm allows us to continue the study of ceramic fibers embedded in ceramic matrix CMCs (C/C, C/SiC, SiC/SiC) as a traditional class of opaque materials. However, at the same time, mullites,  $\text{Al}_2\text{O}_3/\text{Al}_2\text{O}_3$  have been reviewed as a class of semitransparent elements for designing CMCs. The relevance of studying the effect of oriented fibers on the formation of thermoradiation and temperature fields in a semitransparent material was noted. Modeling the scattering asymmetry coefficient influence (scattering phase function) on the generation of the subsurface thermal radiation source was carried out. The methodology for calculating the thermoradiative field in a semitransparent medium (with relative absorption, scattering indexes, and scattering asymmetry coefficient) was used under a one-dimensional two-flux model as the first approximation for solving the radiative heat transfer equation. Calculations of temperature profiles in opaque and semitransparent ceramics were presented under heat load typical for the combustion chambers operating regime of diesel and gas turbine engines.

**Keywords:** ceramics; EBC; TBC; phase scattering function; semitransparent; asymmetry; zirconia; subsurface temperature maximum



**Citation:** Merzlikin, V.; Safonov, E.; Kostyukov, A.; Parshina, S.; Dokukina, A. Affect of the Scattering Asymmetry by Structural Element of Thermal- or Environmental-Barrier Ceramics on Subsurface Radiant Overheating. *Ceramics* **2023**, *6*, 717–733. <https://doi.org/10.3390/ceramics6010044>

Academic Editor: Gilbert Fantozzi

Received: 1 December 2022

Revised: 8 February 2023

Accepted: 8 March 2023

Published: 13 March 2023



**Copyright:** © 2023 by the authors. Licensee MDPI, Basel, Switzerland. This article is an open access article distributed under the terms and conditions of the Creative Commons Attribution (CC BY) license (<https://creativecommons.org/licenses/by/4.0/>).

## 1. Introduction

Thermal Barrier Coating (TBC) systems continue to be one of the key material technologies that offer a great benefit to the operation of gas turbine aircraft engines, gas turbine shipboard engines, land-based industrial gas turbine engines [1–4], and recently renewed interest in the use of ceramics in diesel reciprocating engines [5]. Zirconia ( $\text{ZrO}_2$ ) is a readily-available material with reasonable processing cost, possessing excellent mechanical, electrical, optical, and wear properties. The fabricated zirconia is used in a wide range of applications not limited to aerospace, automotive, medical, and military.

Despite the apparent success of traditional developments of TBC (using zirconium dioxide), many studies have already been dedicated to the multi-disciplinary nature application of the thermal barrier materials (and coatings on their basis), whose properties are also relevant for the development of environmental coatings.

The International Engineering Conferences (devoted to Thermal and Environmental Barrier Coatings) held in 2022 [6] attempted to bring together those who have expertise in specific aspects:

- involved materials,
- processing with conventional and innovative methods,
- processes control of mechanics and chemistry degradation,
- developments of newer materials as alternatives to yttria-stabilized zirconia,
- monitoring of high-temperature oxidation and corrosion including calcia–magnesia–alumina–silicate (CMAS) attack,
- impact of convective and radiative heat transport,
- influence of diffusion, high-temperature creep, and sintering phenomena
- carrying out engineering design [6–9].

More recently, Environmental Barrier Coatings (EBC) that protect silicon-based ceramic matrix composites and alloys (using silicon-based ceramic matrix) have become an area of accelerating materials research.

It is noteworthy that research on TBC and EBC has accelerated greatly over the past twenty years and that this research has resulted in the commercial and military use of new bond coats, low thermal conductivity coatings, coatings that resist degradation induced by environmental deposits ingested into the engine, and also the introduction of EBC into service industrial gas turbine engines and reciprocating engines [1].

Analysis of publications over the past 10 years showed that, as before, researchers have not paid attention to the radiant heat transfer and the influence of the optical characteristics of semitransparent ceramic heat-insulating materials such as zirconium dioxide (for classical TBCs), matrix ceramic structures using mullites, or  $\text{Al}_2\text{O}_3/\text{Al}_2\text{O}_3$  for the development of a new class of highly reflective CMCs being a part of the advanced EBC.

CMCs as ceramics with fibers embedded in a ceramic matrix (C/C, C/SiC, SiC/SiC, and other similar components) remain by their optical properties the typical opaque materials for radiation in the wavelength range  $\sim 0.4\text{--}4\ \mu\text{m}$  produced under ICE and GTE operating conditions or, for example, other exotic radiation sources such as laser irradiation (exposure).

For example, the authors of [9] conducted an integrative review of the biological and mechanical outcomes of porous zirconia structures for extensive bone repair. The presented review, of course, required the inclusion of extensive developments on the evaluation of optical characteristics for the selection of laser processing modes for dental implants in terms of finishing polishing and grinding of ceramic crowns [10].

Currently, there is a trend to use new ceramic and composite materials and coatings in engines. In order to improve the efficiency of gas turbine engines, developers seek to raise the gas temperature in front of the turbine, for which high-temperature alloys and materials are actively used. This is especially important considering the presence of the radiant component up to 30–40% in the integral heat flux up to hundreds of  $\text{kW}/\text{m}^2$  [11]. On the basis of these materials, at present, the best effort has been made in a microturbine power plant Aurelia A400 with an electrical efficiency of 40% [12].

It should also be noted that the partial transparency of the coatings of the elements in the flow path of gas turbine engines (combustion chambers and turbine rotor blades) has a significant effect on reducing the temperature gradient in the materials of multilayer coatings and, as a result, increasing the service life of the coatings [13–23].

There is another effect and advantage of using semitransparent materials. This phenomenon consists of the shift of even the temperature profile maximum from the irradiated surface into the depths of scattering multilayer materials of thermal and environmental barriers [17,19–21].

The stable operation of GTE elements with coatings is prevented by degradation caused by the ingress of deposits from the environment into the engine.

Upon entering the GTE hot section, small/fine particulates begin to melt, impinge, and adhere to the thermal barrier coatings/materials (TBC/TBM) and can infiltrate the porous

coatings, solidifying and forming the glassy calcia-magnesia-alumino-silicate (CMAS) coating, which can degrade the TBC properties.

It was supposed that there is a degradation of optical characteristics for TBC in combination with EBC which caused a decrease in the resistance to the significant radiant component (up to 50%) of the intense flux of penetrating IR radiation.

However, as laboratory tests have testified [23,24], the produced compositions of  $\text{CaO}:\text{Al}_2\text{O}_3:\text{SiO}_2$  (CMAS) have low radiation absorption in the range of 0.3–5  $\mu\text{m}$ , which is an optical characteristic not worse than for porous samples. It was experimentally shown that the transmittance of a two-millimeter sample with a different weight content of silica reaches ~60–90% in the indicated wavelength range [25].

Thus, it should be considered that a significant change in thermomechanical properties is caused by the deposition of highly absorbing microparticles, but other various foreign bodies with high absorption in the spectrum of intense affecting IR radiation. As a result, the absorption of the radiative component can increase by several times. In this case, the convective heating of the exposed surface does not change.

In some works, it was observed that in certain ceramic systems, including SiC, silicon nitride,  $\text{Al}_2\text{O}_3/\text{Al}_2\text{O}_3$  processes of anomalous grain growth take place which can lead to microstructure formation, demonstrating elongated large grains in a matrix of smaller rounded grains [23,26–28].

For semitransparent materials, this thermophysical effect of self-sustaining fiber generation and grain growth is an example indicating the need to start studying the effect of fiber orientation on the formation of thermal radiant fields.

Thus, anisotropic properties appear following the orientation of fibers.

This effect is a special case of studying directed scattering by elements of an optically inhomogeneous medium, which makes it possible to control and manage with radiant and temperature fields.

The aim of this study is to solve these problems.

The authors of this paper present a methodology for modeling these fields using dependence on absorption and scattering indices and the variability of the symmetry coefficient (the shape of the scattering phase function) for the structural elements of a semitransparent material.

## 2. Materials and Methods

### 2.1. Radiation Thermophysics of Semitransparent Materials as a Tool for Modeling and Improving Multifunctional Characteristics of TBC and EBC

The authors aim to show the possibility of controlling thermal modes within subsurface zones of TBC/EBC based on semitransparent materials (coatings) in comparison with traditional opaque heat-insulating ones.

Currently-used engineering or structural ceramics (crystalline inorganic non-metallic materials) in aerospace include ceramic thermal and environmental barrier coatings for protecting hot section components of aircraft turbine engines from high heat flux in high-temperature combustion environments, rocket exhaust nozzles, and thermal protection systems for space vehicles [1–5,22,25–30].

This problem has been relevant for the development of internal combustion engines and GTE elements using traditional semitransparent porous ceramic materials for many decades [15–21,30–34].

Ceramic matrix composites (CMC), including non-oxide and oxide CMC, are also being incorporated in turbine engines in high-pressure and high-temperature section components and turbine exhaust nozzles with long-duration design operating lifetimes.

Many authors point out that ceramic materials have many attributes that make them excellent heat-insulating materials for high temperatures and ultra-high temperatures.

Regarding protective coatings and structural materials, the current uses have been limited due to their low toughness, large variability in mechanical properties, and complex environmental effects in harsh operating conditions.

It should be noted that in recent years engineers have not always covered such important characteristics for TBC/EBC, as semitransparency causes scattering and absorption of external radiant action for ICE and GTE [29–34].

At high temperatures in combustion chambers, red-hot soot particles (in the composition with hot gas flows) generate radiation (in the visible and IR ranges of the spectrum) with power density values, respectively, up to hundreds of  $\text{kW}/\text{m}^2$  [11] for gas-turbine engines and several  $\text{MW}/\text{m}^2$  [31–34] for diesel ones.

Ceramic matrix composites are a subgroup of composite materials and a subgroup of ceramics. They consist of ceramic fibers embedded in a ceramic matrix. The fibers and the matrix both can consist of any ceramic material, whereby carbon and carbon fibers can also be regarded as ceramic materials.

Carbon, special silicon carbide, and others are the first class of opaque materials.

Semitransparent ones based on alumina ( $\text{Al}_2\text{O}_3$ ), stabilized zirconia ( $\text{Zr}_2\text{O}_3$ ), and mullite (industrial pottery  $\text{Al}_2\text{O}_3\text{--SiO}_2$ ) are considered the second class of scattering media within the range of transparency  $\sim 0.4\text{--}4\ \mu\text{m}$  of the affecting radiation.

The important commercially available CMCs are:

- highly absorbent materials C/C, C/SiC, SiC/SiC,
- weakly absorbing materials for TBC/EBC manufactured on the basis of less common substances alumina, stabilized zirconia, and mullite.

They differ from conventional ceramics. All of these materials commonly could be used for CMCs for both classes of substances depending on the spectrum of the radiant component of the integral heat flux including the convective one.

The main differences in the methods for calculating thermoradiation and temperature fields are as follows:

- (1) semitransparent materials produce a short-wavelength thermal radiant source within the subsurface region of the exposed TBC/EBC sample, which leads to the use of an inhomogeneous heat conduction equation with boundary absorption of convective fluxes together with intrinsic radiation in long-wavelength radiant flux (according to Planck's law) for the external environment and the heated exposed surface;
- (2) opaque materials absorb the short-wavelength radiant flux on the irradiated surface of the TBC/EBC sample in addition to the boundary conditions according to p.1.

Thus, the calculations according to p.1 require a special technique for calculating the absorbed energy depending on the structure of the semitransparent material, which determines the effects of scattering and absorption.

Radiation thermophysics of semitransparent materials as tooling for modeling and improving multifunctional ceramics TBC and EBC.

Heat transfer by thermal radiation in semitransparent materials at high temperatures is very important and even dominant. An accurate prediction of temperature and heat flux response to rapid heating of any structure made of semitransparent ceramics requires a solution of the coupled radiative and conductive heat transfer problem.

To solve this problem, it is necessary to know the optical properties of ceramics, which depend on the properties of the charge material and the ceramic microstructure. Thus, to estimate the optical characteristics in the framework of the G. Mie scattering theory (the direct problem), it is sufficient to know the relative complex refractive index and the distribution function of the number of pores on their size.

The relative complex refractive index (in particular, air pores) is given by

$$m = 1/(n + i \cdot \chi), \quad (1)$$

where  $n$  is the absolute refractive index,  $\chi$  is the dimensionless absorption indicator at the imaginary unit  $i$ .

The distribution function  $N(D)$  of the number of the pores (concentration of scatterers per volume unit,  $\text{m}^{-3}$ ) by effective size  $D$  is determined using the relationship  $dN(D)/dD$  ( $\text{m}^{-4}$ ).

The direct use of the G. Mie theory is a very difficult task for estimating the characteristics of a thermoradiation field (in particular, the function of a thermal radiation source) to ensure a classical solution of the heat conductivity equation.

Therefore, the independent approximate solution is traditionally considered for the radiative transfer equation within the inverse problem, which takes into account the processes of scattering, absorption, and thermal emission. These processes are identified by photometric measurements of hemispherical reflectance and transmission coefficients, which make it possible to calculate the integral absorption and scattering indices. However, the value of these indicators becomes uncertain without taking into account the scattering phase function, which practically cannot be measured experimentally.

Therefore, for an indirect interpretation of the phase scattering function, this paper uses a one-dimensional model of the scattering phase function  $p(\vartheta)$  according to the scattering angle  $\vartheta$ . Then, taking into account the spatial structure of the phase function, the hemispherical scattering index  $\sigma^+$  in the direction of the incident radiation (front hemisphere) is introduced (under conditions of azimuthal symmetry):

$$\sigma^+ = 2\pi \times \sigma \int_0^{\pi/2} p(\vartheta) d\vartheta, \quad (2)$$

where  $\sigma$  is the integrated scattering index,  $\vartheta$  is the polar scattering angle.

The phenomenological model used in this paper for solving the radiant heat transfer equation assumes introducing the asymmetry parameter of the scattering phase function, as a fraction of the radiation scattered “backward”—towards the incident radiation:

$$\beta = \frac{\int_{\pi/2}^{\pi} p(\vartheta) d\vartheta}{\int_0^{\pi} p(\vartheta) d\vartheta}, \quad (3)$$

For a spherical scattering phase function  $\beta = 1$ .

All these phenomena are also characterized by the spectral dependence of the considered scattering and absorption characteristics and by the scattering phase function.

When modeling the structural composition, it is possible to achieve spectrally selective reflected, absorbed, and transmitted radiation for a ceramic layer with a given optical inhomogeneity (porosity).

Then the temperature field formed in the thickness of the ceramic can generate a certain spectral mode of emission of thermal radiation.

## 2.2. The Phenomenological Model of Radiation-Conductive Heating for Scattering and Absorbing Materials

Let us present the general radiative transfer equation and its solution in one-dimensional approximation for radiant flux  $q(z)$  within the framework of the phenomenological approach. If the medium is optically homogeneous and semitransparent in the sense that there is only absorption in the volume, then there is an extinction according to the Bouguer law.

In the case of semitransparent and scattering media, an additional source of radiation appears in the energy conservation equation from scattering particles (pores) surrounding the elementary volume of the turbid media. To take this into account, it is necessary to add (for a given direction of radiation propagation) the energy determined by the scattering of radiation within some point of the elementary volume, but in a certain direction.

In the same equation, the function of thermal sources of self-radiation will not be taken into account according to Planck’s law.

The boundary conditions will be determined by the incident radiation on the exposed surface.

Hereafter, we will not take into account the spectral dependence.

The simplified model should contribute to the development of predictive estimates of the thermal modes and recommendations on the main directions of research for the radia-

tion thermophysics of semitransparent materials, for example, ceramics in the composition of TBCs or EBCs.

In this work, to solve the complete radiative transfer equation, a two-flux model of radiation propagation was used with an estimate of the influence of the scattering phase function, but in a one-dimensional approximation.

Many authors also follow this approximation, but even for engineering estimates, as a rule, they confine themselves to the spherical scattering indicatrix [18,19,21,31–34].

We will assume that the processes of absorption and scattering occurs on a certain segment in the direction  $z$  of the propagation of the incident monochromatic radiation flux (“forward”), as well as in the opposite direction (“backward”).

Let us introduce the following optical phenomenological parameters of a semitransparent material in a one-dimensional approach:

- (1) model asymmetry coefficient  $\beta$  is the fraction of single scattering (reflection) towards the propagating beam of oppositely directed radiant fluxes  $q(z)$ ;
- (2) instead of the radiation flux  $q(z)$  fixed at the depth of material, the following ones are introduced:  $q_1(z)$  is the flux propagating along the axis (“forward”), and  $q_2(z)$ —the flux—in the opposite direction to  $q_1(z)$ , towards the incident flow  $q_0$  (“backward”);
- (3)  $\omega = \sigma/(\kappa + \sigma)$  is the probability of “survival” of a radiation quantum during the passage of the elementary length  $dz$  (albedo of the single scattering).

For porous materials, the boundary reflection can be neglected. This means that for monolithic semitransparent (scattering and absorbing) materials, the reflectivity (volume reflection) significantly exceeds the boundary reflection coefficient according to the Fresnel law.

Then, for the mutually opposite directions of propagation of fluxes  $q_1(z)$  and  $q_2(z)$ , the formed functions of thermal radiant sources (without taking into account self-radiation), respectively, are equal [17,19,21,31,32]:

$$E_1(z) = (1 - \beta)\omega \times q_1(z) + \beta\omega \times q_2(z), \tag{4}$$

$$E_2(z) = (1 - \beta)\omega \times q_2(z) + \beta\omega \times q_1(z), \tag{5}$$

The classical radiative transfer equation is presented as a system of two ordinary differential equations for the radiation flux, which depends on the variable, the optical thickness  $s = (\kappa + \sigma) \cdot z$ :

$$dq_1/ds = -q_1(s) + \omega(1 - \beta) \times q_1(s) + \beta\omega \times q_2(s), \tag{6}$$

$$dq_2/ds = -q_2(s) + \omega\beta \times q_1(s) + (1 - \beta)\omega \times q_2(s). \tag{7}$$

Boundary data:

- frontal exposed surface  $s = 0$

$$q_1(s = 0) = q_{01}, \tag{8}$$

- back surface of a plane-parallel semitransparent plate (possibly exposed from reflection by the substrate) with optical thickness  $s_0 = (\kappa + \sigma) \cdot z_0$

$$q_2(s = s_0) = q_{02}. \tag{9}$$

To solve the system of Equations (6) and (7), new functions are introduced that have a definite physical meaning:

- duplicated the average radiation intensity

$$J = q_1 + q_2, \tag{10}$$

- radiation flux absorbed by a semitransparent layer with thickness  $ds$

$$H = q_1 - q_2. \tag{11}$$

Then from Equations (6) and (7) we obtain:

$$dH/ds = -(1 - \omega) \times J, \tag{12}$$

$$dJ/ds = -[1 - \omega \times (1 - \beta)] \times H. \tag{13}$$

From here it follows that:

$$d^2J(s)/ds^2 = -k^2 \times J(s), \tag{14}$$

where the normalized deamplification index  $k$  for the scattering and the absorbing material is given by:

$$k = \sqrt{(1 - \omega) \times [1 - \omega(1 - 2\beta)]}. \tag{15}$$

The solution to Equation (14) is

$$J(s) = C_1 \times e^{ks} + C_2 \times e^{-ks}. \tag{16}$$

Taking into account the boundary data (8) and (9) an analytical form for the fluxes  $q_1(s)$  and  $q_2(s)$  is:

$$q_1(z) = \frac{1}{1 - A^2 \times \exp(-2k(\kappa + \sigma)z_0)} \left\{ [q_{02} - q_{01}Ae^{-k(\kappa + \sigma)z_0}] Ae^{-k(\kappa + \sigma)(z_0 - z)} + [q_{01} - q_{02}Ae^{-k(\kappa + \sigma)z_0}] \times e^{-k(\kappa + \sigma)z} \right\}, \tag{17}$$

$$q_2(z) = \frac{1}{1 - A^2 \times \exp(-2k(\kappa + \sigma)z_0)} \left\{ [q_{02} - q_{01}Ae^{-k(\kappa + \sigma)z_0}] \times e^{-k(\kappa + \sigma)(z_0 - z)} + [q_{01} - q_{02}Ae^{-k(\kappa + \sigma)z_0}] \times A \times e^{-k(\kappa + \sigma)z} \right\}, \tag{18}$$

where  $A$  is the reflection coefficient (albedo) for a half-infinite layer of a semitransparent material ( $z_0 = \infty$ ):

$$A = \frac{k - 1 + \omega}{k + 1 - \omega} = \frac{\sqrt{\kappa^2 + 2\beta \times \sigma \times \kappa} - \kappa}{\sqrt{\kappa^2 + 2\beta \times \sigma \times \kappa} + \kappa}. \tag{19}$$

An analysis of the obtained expressions for radiant fluxes shows that the quantity  $b = k(\kappa + \sigma)$  represents the index extinction

$$b = k \times (\kappa + \sigma) = \sqrt{\kappa^2 + 2\beta \times \sigma \times \kappa} \tag{20}$$

for penetrating radiation in the subsurface volume, but within the framework of a one-dimensional model and as a first approximation for solving the classical radiative transfer equation.

Assuming

$$q_{01}(z = 0) = q_0, q_{02}(z = z_0) = 0 \tag{21}$$

and neglecting its long-wave radiation, you can find these coefficients, using the following relationships:

$$r(z_0) = \frac{q_2(z = 0)}{q_0}, \tau(z_0) = \frac{q_1(z = z_0)}{q_0}, a(z_0) = \frac{q_1(z_0) - q_2(0)}{q_0} \tag{22}$$

Then the new phenomenological formulas for  $\kappa$  and  $A$  determine reflection  $r(z_0)$ , transmission  $\tau(z_0)$ , and absorption  $a(z_0)$  coefficients due to radiative extinction by flat plate  $z_0$  for corresponding expressions in full or short forms:

$$r(z_0, \kappa, \sigma, \beta) = \frac{\left[1 - e^{-2 \cdot (\sqrt{\kappa^2 + 2\beta \times \sigma \times \kappa}) \cdot z_0}\right] \times \left(\frac{\sqrt{\kappa^2 + 2\beta \times \sigma \times \kappa - \kappa}}{\sqrt{\kappa^2 + 2\beta \times \sigma \times \kappa + \kappa}}\right)}{1 - \left(\frac{\sqrt{\kappa^2 + 2\beta \times \sigma \times \kappa - \kappa}}{\sqrt{\kappa^2 + 2\beta \times \sigma \times \kappa + \kappa}}\right)^2 \times e^{-2 \cdot (\sqrt{\kappa^2 + 2\beta \times \sigma \times \kappa}) \cdot z_0}}, \tag{23}$$

$$\tau(z_0, \kappa, \sigma, \beta) = \frac{(1 - A^2) \times e^{-b \times z_0}}{1 - A^2 \times e^{-2 \times b \times z_0}}, \tag{24}$$

$$a(z_0, \kappa, \sigma, \beta) = (1 - A) \frac{1 - e^{-b \times z_0}}{1 + A e^{-b \times z_0}}. \tag{25}$$

By differentiating the absorbed flux  $H(z, z_0)$  with respect to the  $z$ -coordinate of the layer  $dz$ , the heat source function can be calculated to ensure a solution to the heat conductivity equation for semitransparent materials:

$$F(z, z_0, \kappa, \sigma, \beta) = \frac{1}{q_0} \frac{\partial [q_1(z, z_0) - q_2(z, z_0)]}{\partial z} \tag{26}$$

The function of a thermoradiation source for coordinate  $z$  of scattering and absorbing plate  $0 \leq z \leq z_0$  of a semitransparent material with a thickness  $z_0$  is:

$$F(z) = q_0 \frac{(1 - A)b}{1 - A^2 \exp(-2bz_0)} \{ \exp(-bz) - A \exp[b(z - z_0)] \} \tag{27}$$

For the case of a semitransparent material with a semi-infinite thickness, the formula is simplified:

$$F(z, z_0, \kappa, \sigma, \beta) = q_0(1 - A)b \times e^{-bz}. \tag{28}$$

A similar formula for calculating the absorbed flux is Bouguer’s law. However, instead of depending on a single absorption index, the proposed formula also takes into account scattering processes. Instead of the boundary reflection coefficient (according to Fresnel’s law) the albedo for the subsurface volume reflection is introduced.

### 3. Results

The optical properties of ceramic materials of studied TBC/EBC appeared to have been poorly studied. These materials, unlike opaque ones, are selectively low absorbing and high scattering media in transparent bands of definite wavelength range during an ignited gas mixture in the combustion chamber of high-speed diesel or gas turbine engines.

The modeling of thermoradiation fields inside the subsurface volume is determined by simple Equations (23)–(28) for computational engineering problems of predicting thermal modes of semitransparent ceramics being a part of multifunctional materials for thermal and environmental protection.

In Tables 1 and 2, the optical and thermal physical characteristics of opaque and semi-transparent samples of partially stabilized zirconium dioxide versus its porosity are presented.

**Table 1.** Thermophysical characteristics for the studied optical models of opaque and semitransparent PSZ ceramics.

Optical Type of Material	Optical Model	Porosity P %	Density $\rho$ kg/m <sup>3</sup>	Conductivity $K_T$ W/m·K
Opaque	M <sub>0</sub>	0	6000	3.0
	M <sub>1</sub>	0	6000	3.0
Semitransparent	M <sub>2</sub>	10	5500	2.5
	M <sub>3</sub> *	8–20	4900	1.5
	M <sub>4</sub>	40	3700	1.0

(\*) Experimental sample.

**Table 2.** Influence of the specified input asymmetry factor  $\beta$ , absorption index  $\kappa$  and integrated scattering one  $\sigma$  on the changes of the optical phenomenological parameters: albedo  $A(\kappa, \sigma, \beta)$  and extinction index  $b(\kappa, \sigma, \beta)$  depending on the optical characteristics of the models  $M_1, \dots, M_4$  for absorbing and scattering ceramics.

Optical Model	Specified Input			
	Indexes		$\beta = 0.2-0.8$	
	Absorption $\kappa, \text{m}^{-1}$	Scattering $\sigma, \text{m}^{-1}$	Estimated Data	
			Albedo %	Extinction Index $b, \text{m}^{-1}$
$M_1$	28	1000	59–77	109–213
$M_2$	14	1000	69–83	76–150
$M_3^*$	~14	~2400	79–89	116–232
$M_4$	14	3000	81–90	130–260

(\*) Experimental sample.

Semitransparent ceramics with an optical model  $M_3$  were experimental samples intended for spectrophotometric (with help of sandblasted aluminum photometric ball) measurements of reflection and transmission coefficients on a unique setup [18] with laser sources of radiation in the range of near-IR radiation up to 4  $\mu\text{m}$ , which is characteristic of a continuous spectrum of red-hot soot particles in the combustion chamber of diesel or gas turbine engines.

Plane-parallel ceramic plates of various thicknesses  $H = 1-10$  mm were molded. Granular powder (from microballoons) of stabilized zirconia ( $\text{ZrO}_2 + 8\% \text{Y}_2\text{O}_3$ ) was mixed with an adhesive binder with a low absorption index (less than  $1 \text{m}^{-1}$ ) and subjected to weak structural pressing in a ring frame.

The resulting samples had sufficient structural strength and withstood laser heating during relative measurements using a spectrophotometric aluminum ball and plate standards (made of quartz ceramics) as certified optical materials.

Further, by solving the system of Equations (23) and (24), we can calculate two pairs of optical parameters characterizing the absorption and scattering properties of a semitransparent material: ( $A$  and  $b$ ) or ( $\kappa$  and  $\beta\sigma$ ).

Table 2 presents the optical data for the spherical scattering phase function with asymmetry factor  $\beta = 0.5$  at absorption index  $\kappa \sim 8-20 \text{m}^{-1}$  and integral scattering index  $\sigma \sim 2200-2600 \text{m}^{-1}$ .

The remaining ceramics in Table 2 were model samples:

- opaque monolithic material with a surface reflection  $r(z_0) = 20\%$  (model  $M_0$ );
- semitransparent materials with the following characteristics:
  - experimental one with a value of absorption index  $\kappa_3 = 14 \text{m}^{-1}$  and different scattering  $\sigma = 1000-3000 \text{m}^{-1}$  (models  $M_2, M_3, M_4$ )
  - modeling one with identical scattering  $\sigma = 1000 \text{m}^{-1}$ , but different absorption  $\kappa_1 = 28 \text{m}^{-1}$  and  $\kappa_2 = 14 \text{m}^{-1}$  (models  $M_1, M_2$ ).

The thermophysical characteristics of these models (thermal conductivity  $K_T$ , density  $\rho$ , porosity  $P$ ) were known reference data.

In Table 2 there are the calculated phenomenological parameters: albedo  $A$  (reflection coefficient of a semi-infinite layer of matter) and the one-dimensional extinction index  $b$  are presented for two asymmetry coefficients  $\beta = 0.2$  and  $0.8$  or the fraction  $(1-\beta)$  of radiation scattered by an elementary structural element of a semitransparent material—“Forescattering” and “Backscatter”.

With the growth of the redistribution of the scattering flux towards the incident radiation  $\beta = 0.2-0.8$  in four times:

- albedo  $A$  increases by  $\sim 10\%$ , and
- extinction index  $b$  increases almost two times.

A similar effect is observed when analyzing changes in the reflection  $r(z, \kappa, \sigma, \beta)$  (23) and transmission  $\tau(z, \kappa, \sigma, \beta)$  (24) coefficients vs. the thickness of a semitransparent material, respectively, due to the influence of absorption for models  $M_1, M_2$  and scattering for models  $M_2, M_3, M_4$  (See Figure 1).

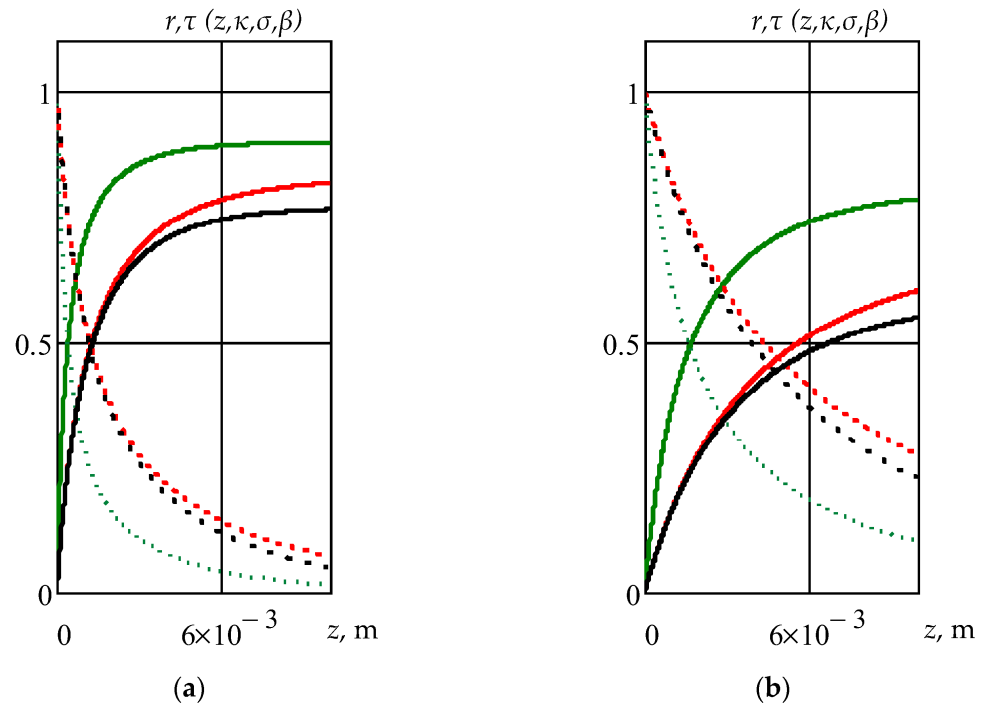


**Figure 1.** Influence of the asymmetry factor  $\beta = 0.8$  (a), and  $0.2$  (b) on the reflection  $r(z)$  (solid lines) and transmission  $\tau(z)$  (dotted lines) coefficients for absorbing and scattering ceramic layer (thickness 0.01 m) with optical models:  $M_1$ —“Black“,  $M_2$ —“Red“,  $M_4$ —“Green“ Lines (See Tables 1 and 2).

Thus, with the same porosity of a semitransparent material, the modeling of optical characteristics is possible by varying the shape and orientation of the elementary structural element without reducing the mass fraction of the substance that determines the structural strength TBC/EBC.

The calculated estimate of the function of a thermal radiant source using formulas (26), (27) makes it possible to calculate the volumetric energy release for penetrating radiation (See Figure 2).

The same optical properties are considered for semitransparent ceramic plates (thickness 0.01 m) under the influence of a model radiant-convective flux up to  $\sim 1.8 \text{ MW/m}^2$  with 50% radiant component characteristic for diesel engine combustion chambers.

Large absorption by ceramics ( $M_1$ ) causes a high value of the absorbed radiation flux density  $F(z, z_0, \kappa, \sigma, \beta)$  on the exposed surface in contrast to the reaction to this heat load of the weakly absorbing material (optical models  $M_2, M_3, M_4$ ), which has the additional property of high scattering.

However, with a decrease in the asymmetry factor  $\beta$  of the structural element (a decrease in the radiation fraction scattered towards the incident radiation flux  $q_0$ ), the absorption of penetrating radiation appears at a greater depth of the semitransparent material. This effect is caused by a large optical path (distance)  $s = (\kappa + \sigma) z$ , which is implemented by a drifting radiation quantum. A large optical path will form an increase with absorption and temperature within the subsurface volume of the scattering material.

The above algorithm for estimating thermoradiation fields in semitransparent materials makes it possible to investigate the impact of the asymmetry of scattering phase function by a structural element of thermal and environmental barrier ceramics on radiant subsurface overheating.

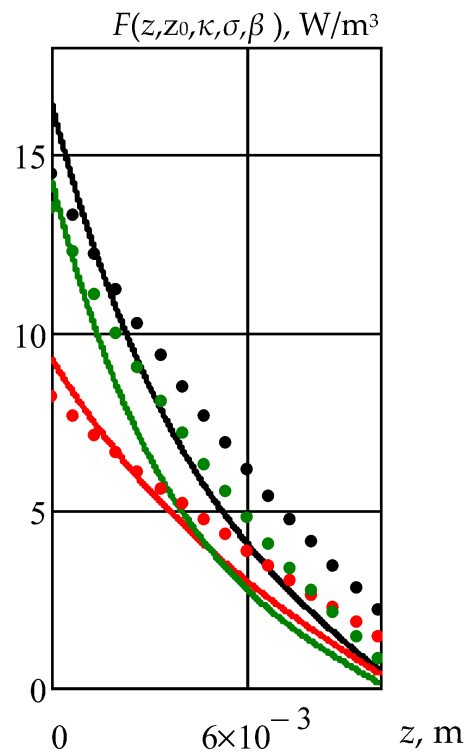


**Figure 2.** One-dimensional distribution of absorbed radiant energy per time and per volume unit  $F(z, z_0, \kappa, \sigma, \beta)$  of short wavelength radiation depending on the coordinate  $z$  in the plate (thickness 0.01 m) of semitransparent ceramics with optical models  $M_1$ —“Black”,  $M_2$ —“Red”,  $M_4$ —“Green” Lines at asymmetry factor  $\beta = 0.8$  (solid lines),  $0.2$  (dashed lines) (See Tables 1 and 2).

Let us use the classical form of the solution of the inhomogeneous heat conductivity equation used in many studies [19,21,31–34], but in which, in explicit form, the calculated estimates of the influence of the approximate one-dimensional phase scattering function were not considered.

The temperature fields are calculated in accordance with the method proposed in [17] for solving the heat equation with an inhomogeneous term in the form represented by formulas (26), (27).

The boundary conditions will be simulated by complex convective and radiant heating of ceramics under total stationary convective-thermoradiant heat flux  $\sim 1.8 \text{ MW/m}^2$  with radiant heat loading  $q_0 = 0.9 \text{ MW/m}^2$  (short-wave range) at a constant temperature 800 K and heat transfer coefficient  $\alpha_{\text{TS}} = 1500 \text{ W/(m}^2 \cdot \text{K)}$  of the external atmosphere; emittance for gas atmosphere  $\varepsilon_A \sim 0.4$  and for exposed plate surface as black body  $\varepsilon_S \sim 1$  (long-wave one); heat transfer coefficient  $\alpha_{\text{Tb}} = 200 \text{ W/(m}^2 \cdot \text{K)}$  for cooled back side of the thermal barrier materials.

Figure 3 shows temperature profiles in the plate (0.01 m thickness) for opaque ceramics (optical model  $M_0$ —dotted lines) with reflection coefficient  $r(z_0) = 20\%$  and semitransparent (solid lines) ceramics with optical models  $M_1, M_2, M_3, M_4$  ( $A \sim 50\text{--}90\%$ ) at scattering asymmetry factor  $\beta = 0.5$  for a structural element of exposed optically inhomogeneous materials in the composition TBC (EBC) under conditions of a typical stationary convective-radiative heat exchange during a heating time up to 0.1 s (inside the combustion chamber of a diesel engine—Figure 1a), and 10 s, 100 s (for the air-gas channel of gas-turbine, Figure 1b,c).

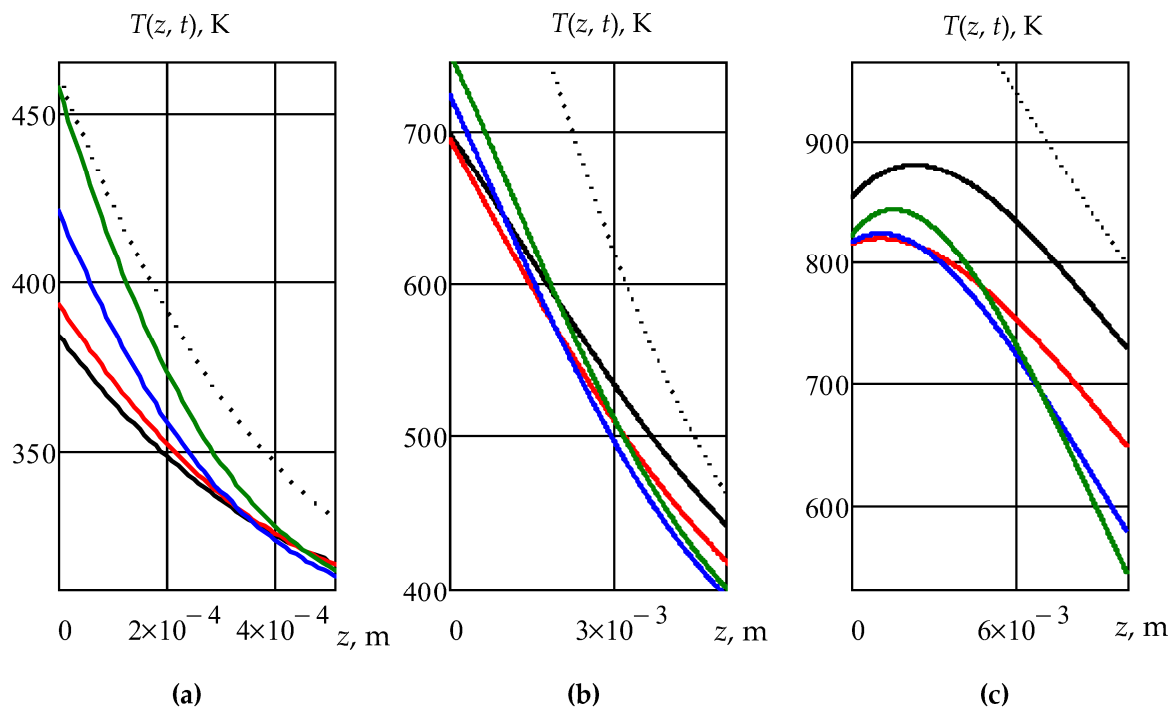


**Figure 3.** Temperature profiles inside the absorbing and scattering plate (0.01 m thickness) for opaque (optical model  $M_0$ —dotted lines) and semitransparent (solid lines) ceramics with optical models  $M_1$ —“Black”,  $M_2$ —“Red”,  $M_3$ —“Blue”,  $M_4$ —“Green” Lines at spherical scattering phase function for a structural element of exposed TBC/EBC sample used for the combustion chamber wall of a diesel engine during the time 0.1 s (a), and for gas turbine one—10 s (b), 100 s (c).

The highest temperature heating of the surface takes place for opaque ceramics (model  $M_0$ , “Black” dotted line, Figure 3) up to 450 K at small times up to 0.1 s and reaches ~1100 K with an increase in the interaction time up to 100 s. This is explained by the fact that an optically opaque material is exposed to a convective-radiant heat flux of up to several MW/m<sup>2</sup> with a model surface absorption of the incident radiant flux of up to ~80% together with the traditional convective component.

In contrast to surface heating of opaque ceramics, the mode of subsurface and deep heating (at long times up to 10–100 s) of semitransparent high- and low-reflective materials changes significantly. The prevailing order of formation of temperature fields on the surface and in depth will be determined by the increase or decrease of albedo at the same value of the absorption indexes  $\kappa_2 \dots \kappa_4 = 14\text{--}28 \text{ m}^{-1}$ .

Highly reflective materials reach lower temperatures of ~500 K (models  $M_3$ ,  $M_4$ —“Blue” and “Green” lines, Figure 3c) in depth (up to 10 mm) in contrast to temperatures of ~700 K for low reflective ceramics (models  $M_1$ ,  $M_2$ —“Black” and “Red” lines, Figure 3c).

For example, the temperature in the range of 670–730 K on the back side of a ceramic plate with low albedo ( $A \sim 60\text{--}80\%$  for models  $M_1$ ,  $M_2$ ) differs by ~100–150 K in comparison to highly reflective materials ( $A \sim 80\text{--}90\%$  for models  $M_3$ ,  $M_4$ ).

The same models produce the appearance of a temperature maximum within subsurface overheating, but in this case, the temperatures for highly reflective materials reach higher temperatures of 850 K (models  $M_4$ —“Green” line, Figure 3c) in comparison to lower temperatures of ~820 K for low reflective materials (models  $M_2$ ,  $M_3$ —“Red”, “Blue” lines, Figure 3c).

A higher value of the maximum temperature for model  $M_1$  (“Black” line, Figure 3c) is achieved for semitransparent ceramics with twice the absorption coefficient  $\kappa_1 = 28 \text{ m}^{-1}$ .

The specified order of formation of temperature fields depending on the albedo of models  $M_1, \dots, M_4$  is preserved when modeling the scattering mode by a structural

element of semitransparent ceramics considering its asymmetry coefficient  $\beta = 0.2\text{--}0.8$  (see Figure 4a–c).

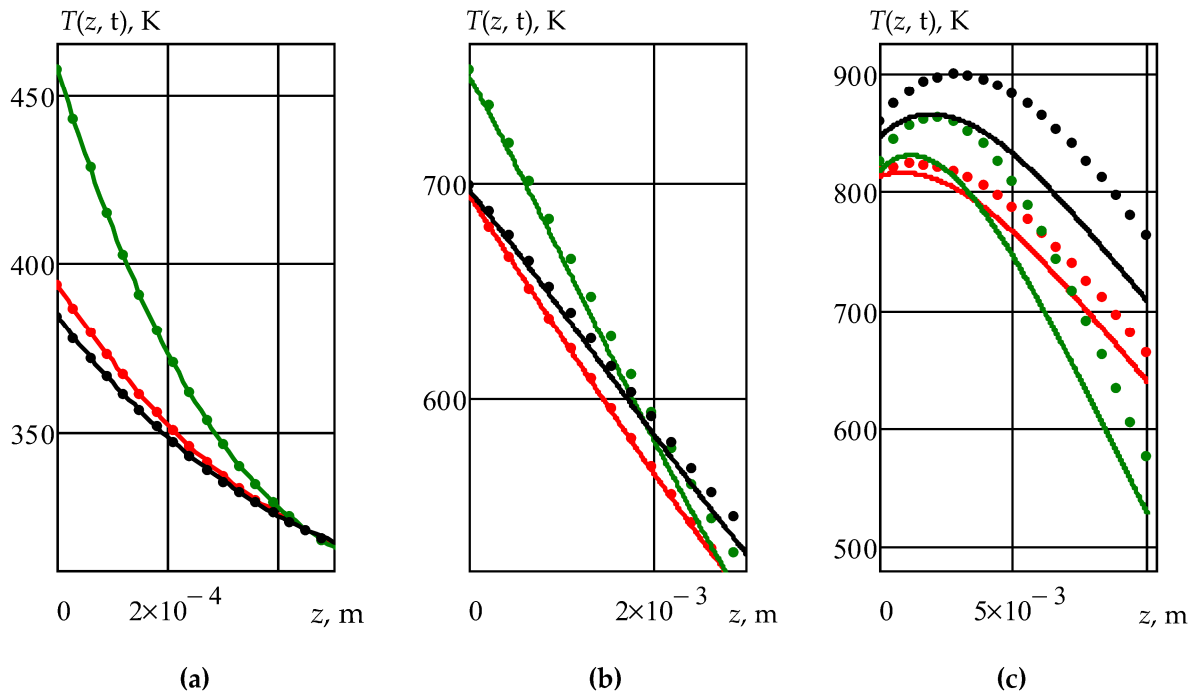


**Figure 4.** Temperature profiles in the absorbing and scattering plate (0.01 m thickness) for opaque (optical model  $M_0$ —dotted lines) and semitransparent (solid lines) ceramics with optical models  $M_1$ —“Black”,  $M_2$ —“Red”, and  $M_4$ —“Green” Lines at asymmetry factor  $\beta = 0.8$  (solid lines) and 0.2 (dotted lines) for a structural element of exposed thermal (environmental) barrier materials during at time 0.1 s (a), 10 s (b), 100 s (c) (see environmental conditions for Figure 3).

The temperature rising in the subsurface zone is caused by the growth of the penetrating radiation scattering in the propagation direction of the incident radiation. This is the so-called forward scattering (“Forescattering”).

The increase in the value of the maximum temperature in the near zone of the subsurface volume amounts to  $\sim 40\text{--}50$  K for the highly reflective model  $M_4$  (“Green” line), due to the large albedo, as well as for the highly absorbing model (“Black” line, Figure 4c).

Thus, depending on the tasks of controlling the temperature fields of semitransparent materials, the modeling of a structural element in the composition of TBC/EBC will allow one to regulate their structural strength, due to the shift of thermal overheating to the subsurface zone of the exposed materials.

#### 4. Discussion

As many authors point out, the considered temperature modes for TBC/EBCs, as well as for their constituent ceramic interlayers, are determined by porosity or a change in the porosity gradient.

The same semitransparent properties are often not even discussed [1–10,13–16].

However, if the ceramics are semitransparent, then in addition to thermal conductivity, one should take into account subsurface radiant heating, which causes volumetric energy release (Figure 2) and even overheating, as shown in Figures 3 and 4.

This effect takes place for the thermal modes of prolonged heating at significant thicknesses of the exposed semitransparent material for tens and hundreds of seconds during operation, for example, of gas turbine engines.

In this case, due to the “freezing” of the temperature rise in the exposed surface, the process of subsurface absorption of penetrating short-wave radiation (generated by red-hot

soot particles) continues effectively at a certain depth, due to competition with the processes of the heat sink to the front or back sides of the heat-shielding material.

With short pulsed heating during a short time up to fractions of a second of the active phase of combustion in the cylinder of a diesel engine, only a decrease in the surface temperature of the exposed walls of the combustion chamber is manifested even at several  $\text{MW}/\text{m}^2$  due to the high reflection coefficient of zirconium, aluminum, silicon dioxide ceramics. Moreover, if absorption (as an isotropic characteristic) depends only on the mass fraction of the substance, then scattering has the property of anisotropy.

As a rule, scattering is also considered a factor due to the porosity or mass concentration of a substance with slightly changing physical properties of ceramics, in particular, with respect to the complex refractive index.

In practice, the effect of porosity on thermal conductivity and integral scattering has the same essence.

However, scattering on the elements of inhomogeneity in the volume of a monolithic material has one more property, namely, differentiated scattering depending on the angle of observation (scattering) on a homogeneous structural element. Therefore, depending on the shape, orientation, and distribution function of scattering elements in a monodisperse semitransparent material, the integral effect of radiation excitation will be different.

For polydisperse media, the effect of angular scattering of randomly located particles of various shapes and sizes will be averaged, and the processes of radiation extinction can be characterized by an integral scattering index. Thus, the structural modeling of a semitransparent material makes it possible to predict the thermoradiation and temperature field within the framework of a certain optical model.

In practice, the measurement of the phase scattering function is not possible except for individual processes, for example, scattering by particles with a spherical scattering indicatrix.

However, the phenomena of anisotropic scattering can be modeled based on measuring hemispherical reflection and transmission coefficients using ordinary spectrophotometers and goniometric setups. The problem of registering the reflection and transmission coefficients using directional radiation sources (laser beams) was solved by the authors in [18].

Then, one can use the one-dimensional approximation of the solution of the radiative transfer equation with a certain asymmetry of the phase scattering function. As shown in Figure 1, the redistribution of scattered energy with the asymmetry factor changing several times changes the reflection and transmission coefficients by 10–20%.

Thus, for material scientists there is a problem of model structuring of ceramic materials, based on the optimal selection of porous materials, using the proposed simple engineering methods for the evaluation of thermoradiation and temperature fields.

## 5. Conclusions

The problem of the formation and characteristics evaluation of a thermoradiant and temperature fields for exposed ceramics Thermal-Environmental-Barrier Coatings (TBC/EBC) has been considered with complex heat transfer, but under the influence of the penetrating intense radiant component.

The authors proposed to analyze not only TBC but also EBC from the point of view of the optics of semitransparent scattering and absorbing media in the range of  $\sim 0.4\text{--}4\ \mu\text{m}$  of external radiant action.

It was assumed by many works that materials produced by CMAS worsen the physical properties of TBC [1–4,26–30]. There is a degradation of the optical characteristics of the TBC in combination with the EBC, which causes a resistance decrease to the intense penetrating IR radiant component of external total heat flux, generated by hot soot particles at the operating conditions for combustion chambers of diesel and gas turbine engines.

The literature analysis showed that the optical characteristics of the formed glassy calcia-magnesia-alumino-silicate (CMAS) have low radiant absorption [24,25] and are similar to weakly-absorbing semitransparent ceramics TBC based on zirconium oxide [17–21].

In this article, the considered optical characteristics of the TBC powder model (as an analog of CMAS) correspond to weakly scattering substance at an insignificant scattering index  $\sigma$  which is not greater the value of the absorption index  $\kappa \sim (8\text{--}20) \text{ m}^{-1}$  ( $\sigma < \kappa$ ).

Thus, using the feature of both TBC and EBC turns factor of the mutual reaction to the significant radiant component in the near IR range (“short-wavelength transparency window” for ceramics).

The study of the development of EBC based on ceramic fibers embedded in a ceramic matrix CMCs shows the relevance of the study influence of orientation and shape of scatterers on processes of scattering (absorption) radiation and, as a consequence, the formation of radiant fields in the subsurface zone of CMCs, already considered as semitransparent media.

The article presents a technique for estimating thermoradiation fields based on a two-flux approach for the solution of the classical radiative transfer equation with an absorption index, total scattering index, integrated over the phase function (indicatrix) scattering with a simulated asymmetry coefficient in a one-dimensional approximation.

To describe the scattering and absorption of radiation fluxes in optically inhomogeneous materials, the following phenomenological parameters have been introduced: albedo  $A(\kappa, \sigma, \beta)$  (the reflection coefficient of a semi-infinite layer of matter) and  $b(\kappa, \sigma, \beta)$ —the extinction index (interpreting the integral one-dimensional scattering and absorption of radiation by the optically inhomogeneous layer).

Calculation and theoretical evolution of temperature profiles in opaque and semitransparent ceramics were carried out under heat load conditions typical for the operating regime of combustion chambers of diesel and gas turbine engines with a total convective-radiative flux up to  $\sim \text{MW}/\text{m}^2$  with a 50% fraction of the radiant component.

The formation of a subsurface temperature maximum for large times and thicknesses of a semitransparent ceramic layer was shown by modeling both the specific scattering  $\sigma/\kappa$  and the asymmetry coefficient  $\beta$  of directed scattering.

The physical meaning of the formation of subsurface overheating in semitransparent materials is due to the emerging heat and energy equilibrium on the exposed boundary. Then, the surface temperature “freezes”, but the internal volume of semitransparent ceramics continues to absorb penetrating short-wave thermal radiation.

A four-fold change in the asymmetry coefficient causes the greatest increase in the temperature profile maximum by  $\sim 50 \text{ K}$  in a ceramic layer 10 mm thick, over a time of up to 100 s at scattering and absorption indexes, equal to  $\sigma \sim 1000 \text{ m}^{-1}$  and  $\kappa \sim 30 \text{ m}^{-1}$  (model M1, Figure 4c), respectively.

Computational estimates of radiant temperature fields during the heating of the thin semitransparent coatings were considered in [17–21,32–34]. The formation of a subsurface temperature maximum for small thicknesses was not observed, but the temperature of the exposed surface decreased significantly. This heating of the ICE ceramic walls causes partial thermal insulation, which led to the designation of this engine as “adiabatic”.

Thus, the effect of partial transparency is especially important and becomes significant using ceramic coatings and materials, for example, for an air-gas channel of turbine engines (combustion chambers and turbine blades).

Due to volumetric heating, a decrease in the temperature gradient takes place and even a positive gradient begins in the near-surface zone of semitransparent materials and coatings is produced. Because of the modeling of TBC/EBC structures, the internal thermal radiation fields can become inverted. This allows one to control and regulate the surface temperature and decrease the subsurface temperature gradient, and as a result, the service life of coatings is increased when interacting with the environment, and the radiation-convective heat load generated by the gas turbine engine.

So, evaluating the radiative properties and their temperature dependence becomes one of the main goals of investigation nowadays.

Another important issue is the study of the influence of structural parameters of ceramic TBC/EBC (porosity, micro-particles, and fibers, their size distribution) on the emitting and radiant properties.

The quantitative relationship between radiative and microstructural properties in combination with the solution to the problem of radiative-conductive heat transfer opens up prospects for the creation of new engineering ceramic structures based on the requirements of the end user for operating conditions of industrial heat power equipment.

The authors note that the article proposes an engineering technique with simple algebraic formulas for calculating thermoradiation and temperature fields for opaque and semitransparent (scattering and absorbing) materials being a part of ceramic thermal or environmental barriers materials and coatings based on it.

**Author Contributions:** Conceptualization: V.M., E.S. and A.K.; Methodology: V.M., E.S. and A.D.; Investigation: V.M. and S.P.; Writing—original draft preparation: S.P., A.D. and E.S.; Writing—Review: S.P. and A.D.; Supervision: S.P., V.M. and A.D. All authors have read and agreed to the published version of the manuscript.

**Funding:** This research received no external funding.

**Institutional Review Board Statement:** Not applicable.

**Data Availability Statement:** Not applicable.

**Conflicts of Interest:** The authors declare no conflict of interest.

## References

1. Nieto, A.; Agrawal, R.; Bravo, L.; Hofmeister-Mock, C.; Pepi, M.; Ghoshal, A. Calcia–magnesia–alumina–silicate (CMAS) attack mechanisms and roadmap towards Sandphobic thermal and environmental barrier coatings. *Int. Mater. Rev.* **2020**, *66*, 451–492. [[CrossRef](#)]
2. Clarke, D.R.; Oechsner, M.; Padture, N.P. Thermal-barrier coatings for more efficient gas-turbine engines. *MRS Bull.* **2012**, *37*, 891–898. [[CrossRef](#)]
3. Lv, B.; Jiang, P.; Li, D.; Wang, T. Advances on the sintering of Thermal Barrier Coatings for high temperature blade of industrial gas turbines. *J. Mater. China* **2020**, *11*, 855–870. [[CrossRef](#)]
4. Nageswara, R.M. Chapter 13: Materials for gas turbines—An Overview. *Advances in Gas Turbine Technology*. In *Advances in Gas Turbine Technology*; Benini, E., Ed.; InTech Open: Rijeka, Croatia, 2011. [[CrossRef](#)]
5. Paul, C.; Fernandez, S.F.; Haworth, D.C.; Roy, S.; Modest, M.F. A detailed modeling study of radiative heat transfer in a heavy-duty diesel engine. *Combust. Flame* **2019**, *200*, 325–341. [[CrossRef](#)]
6. International Engineering Conferences. Thermal and Environmental Barrier Coatings VI. 19–24 Jun 2022 (ECI), Germany Kloster Irsee. Available online: <https://engconf.us/conferences/materials-science-including-nanotechnology/thermal-and-environmental-barrier-coatings-vi/#header0.221122> (accessed on 30 November 2022).
7. Li, G.-R.; Yang, G.-J. Structure Evolution of Multiscaled Thermal Barrier Coatings During Thermal Exposure. *Adv. Nanomater. Coat. By Therm. Spray* **2019**, *Chapter 7*, 221–255. [[CrossRef](#)]
8. Tejero-Martin, D.; Bennett, C.; Hussain, T. A review on environmental barrier coatings: History, current state of the art and future developments. *J. Eur. Ceram. Soc.* **2020**, *41*, 1747–1768. [[CrossRef](#)]
9. Resende-Gonçalves, C.I.; Sampaio, N.; Moreira, J.; Carvalho, O.; Caramês, J.; Manzaneres-Céspedes, M.C.; Silva, F.; Henriques, B.; Souza, J. Porous Zirconia Blocks for Bone Repair: An Integrative Review on Biological and Mechanical Outcomes. *Ceramics* **2022**, *5*, 161–172. [[CrossRef](#)]
10. Han, J.; Zhang, F.; Van Meerbeek, B.; Vleugels, J.; Braem, A.; Castagne, S. Laser surface texturing of zirconia-based ceramics for dental applications: A review. *Mater. Sci. Eng. C* **2021**, *123*, 112034. [[CrossRef](#)]
11. Dannecker, R.; Noll, B.; Hase, M.; Krebs, W.; Schildmacher, K.-U.; Koch, R.; Aigner, M. Impact of radiation on the wall heat load at a test bench gas turbine combustion chamber: Measurements and CFD simulation. In Proceedings of the ASME Turbo Expo Power for Land, Sea, and Air, Montreal, QC, Canada, 14–17 May 2007.
12. Aurelia Turbines Company. The Most Efficient Small Gas Turbines in the World. Available online: <https://aureliaturbines.com/> (accessed on 11 November 2022).
13. Pyatov, I.S.; Makarov, A.R.; Kostyukov, A.V.; Smirnov, S.V.; Posedko, V.N.; Finkelberg, L.A.; Kostyuchenkov, A.N. Prospects for the use of carbon materials for the manufacture of parts for gas turbine engines and reciprocating internal combustion engines (Perspektivy ispol'zovaniya uglerodnykh materialov dlya izgotovleniya detalej gazoturbinykh dvigatelej i porshnevnykh dvigatelej vnutrennego sgoraniya). *Tract. Agric. Mach.* **2015**, *6*, 22–25. (In Russian)
14. Moskal, G.; Mendala, B. Characterization of microstructure and properties of TBC systems with gradient of chemical composition and porosity. *Arch. Metall. Mater.* **2008**, *53*, 945–954.

15. Das, D.; Majumdar, G.; Sen, R.S.; Ghosh, B.B. Evaluation of combustion and emission characteristics on diesel engine with var-ying thickness of PSZ coated piston crown. *Int. J. Innov. Res. Sci. Eng. Technol.* **2013**, *2*, 4858–4865.
16. Uchida, N.; Osada, H. A New Piston Insulation Concept for Heavy-Duty Diesel Engines to Reduce Heat Loss from the Wall. *SAE Int. J. Engines* **2017**, *10*, 2565–2574. [[CrossRef](#)]
17. Merzlikin, V.G.; Bystrov, A.; Minashkin, V.; Marynenko, V.N.; Zagumennov, F. Thermal Mode Optimization of Combustion Chamber Walls for Power-Plants Using Semitransparent Porous Ceramics. *Coatings* **2020**, *10*, 252. [[CrossRef](#)]
18. Merzlikin, V.G.; Bystrov, A.V.; Smirnov, S.V. Detection technique of the optical and thermoradiative characteristics with compensation effect of reflection and transmittance indicatrices for the semitransparent materials with high subsurface scattering. *IOP Conf. Series: Mater. Sci. Eng.* **2019**, *613*, 012049. [[CrossRef](#)]
19. Siegel, R.; Spuckler, C.M. Analysis of thermal radiation effects on temperatures in turbine engine thermal barrier coatings. *Mater. Sci. Eng. A* **1998**, *245*, 150–159. [[CrossRef](#)]
20. Wang, J.I.; Eldridge, S.M.; Guo, F. Comparison of different models for the determination of the absorption and scattering coefficients of TBCs. *Acta Mater.* **2013**, *64*, 402–409. [[CrossRef](#)]
21. Manara, J.; Arduini-Schuster, M.; Rätzer-Scheibe, H.-J.; Schulz, U. Infrared-optical properties and heat transfer coefficients of semitransparent thermal barrier coatings. *Surf. Coat. Technol.* **2009**, *203*, 1059–1068. [[CrossRef](#)]
22. Mironov, R.; Zabezhalov, M.; Cherepanov, V.; Rusin, M.Y. Transient radiative-conductive heat transfer modeling in constructional semitransparent silica ceramics. *Int. J. Heat Mass Transf.* **2018**, *127*, 1230–1238. [[CrossRef](#)]
23. Shamparov, E.; Rode, S.; Bugrimov, A.; Zhagrina, I. Analytical Solution of Problems about the Radiative and Radiative-Conductive Stationary Heat Transfer in a Medium with an Arbitrary Dependence of the Scattering and Absorption on Frequency Boundary Conditions. *Energies* **2021**, *14*, 6339. [[CrossRef](#)]
24. Adilova, V.S.; Spiridonov, Y.A.; Sigaev, V.N. Synthesis and research of the translucent Magnesium Aluminosilicate glass ceramics for the low-Temperature ion exchange. *Achiev. Chem. Chem. Technol.* **2019**, *33*, 34–36. (In Russian)
25. Steimacher, A.; Astrath, N.; Novatski, A.; Pedrochi, F.; Bento, A.; Baesso, M.; Medina, A. Characterization of thermo-optical and mechanical properties of calcium aluminosilicate glasses. *J. Non-Cryst. Solids* **2006**, *352*, 3613–3617. [[CrossRef](#)]
26. Simon, R.A. Progress in Processing and Performance of Porous-Matrix Oxide/Oxide Composites. *Int. J. Appl. Ceram. Technol.* **2005**, *2*, 141–149. [[CrossRef](#)]
27. Shvydyuk, K.O.; Nunes-Pereira, J.; Rodrigues, F.F.; Silva, A.P. Review of Ceramic Composites in Aeronautics and Aerospace: A Multifunctional Approach for TPS, TBC and DBD Applications. *Ceramics* **2023**, *6*, 195–230. [[CrossRef](#)]
28. Merrill, G.B.; Morrison, J.A. High Temperature Insulation for Ceramic Matrix Composites. U.S. Patent 6013592A, 11 January 2020.
29. Zhu, D. *Aerospace Ceramic Materials: Thermal, Environmental Barrier Coatings And Sic/Sic Ceramic Matrix Composites for Turbine Engine Applications*; NASA: Washington, DC, USA, 2018; NASA Langley Research Center, STI Program, Hampton, VA 23681-2199.
30. Liu, Q.; Huang, S.; He, A. Composite ceramics thermal barrier coatings of yttria stabilized zirconia for aero-engines. *J. Mater. Sci. Technol.* **2019**, *35*, 2814–2823. [[CrossRef](#)]
31. Boehringer, J.C.; Spindler, R.J. Radiant heating of semitransparent materials. *AIAA J.* **1963**, *1*, 84–88. [[CrossRef](#)]
32. Merzlikin, V.; Parshina, S.; Marynenko, V. Universal Effect of Subsurface Thermal Radiant Overheating for Semitransparent Materials and Natural Media. In Proceedings of the 7th International Conference on Industrial Engineering (ICIE 2021), Sochi, Russia, 17–21 May 2021; pp. 818–824. [[CrossRef](#)]
33. Merzlikin, V.; Sidorov, O.; Ojeda, M.G.; Amelenkov, A.; Sutugin, V. *Study of Optical Parameters of Semitransparent Materials for Heat-Insulating Coatings of Combustion Chamber*; SAE Technical Papers; SAE International: Rome, Italy, 2007. [[CrossRef](#)]
34. Merzlikin, V.G.; Parshina, S.A.; Garnova, V.Y.; Bystrov, A.V.; Makarov, A.R.; Khudyakov, S.V. Rig test of diesel combustion chamber with piston coated optically simulated semitransparent PSZ-ceramic. SAE Technical Papers, Paper 17ICE-0103/2017-24-0129. In Proceedings of the 13th International Conference on Engines and Vehicle, Capri, Italy, 10–14 September 2017; pp. 168–169. [[CrossRef](#)]

**Disclaimer/Publisher’s Note:** The statements, opinions and data contained in all publications are solely those of the individual author(s) and contributor(s) and not of MDPI and/or the editor(s). MDPI and/or the editor(s) disclaim responsibility for any injury to people or property resulting from any ideas, methods, instructions or products referred to in the content.